OPEN ACCESS

ORIGINAL ARTICLE

Increased ectodomain shedding of lung epithelial cell adhesion molecule 1 as a cause of increased alveolar cell apoptosis in emphysema

Takahiro Mimae,[1,2] Man Hagiyama,[3] Takao Inoue,[3] Azusa Yoneshige,[3] Takashi Kato,[3] Morihito Okada,[1] Yoshinori Murakami,[2] Akihiko Ito[3]

▶ Additional material is published online only. To view please visit the journal online (http://dx.doi.org/10.1136/thoraxjnl-2013-203867).

[1]Department of Surgical Oncology, Research Institute for Radiation Biology and Medicine, Graduate School of Biomedical Sciences, Hiroshima University, Hiroshima, Japan
[2]Division of Molecular Pathology, Department of Cancer Biology, Institute of Medical Science, University of Tokyo, Tokyo, Japan
[3]Department of Pathology, Faculty of Medicine, Kinki University, Osaka, Japan

Correspondence to
Dr A Ito, Department of Pathology, Faculty of Medicine, Kinki University, 377-2 Ohno-Higashi, Osaka-Sayama, Osaka 589-8511, Japan; aito@med.kindai.ac.jp

TM and MH contributed equally to this work.

Received 15 May 2013
Revised 22 August 2013
Accepted 11 September 2013
Published Online First 3 October 2013

ABSTRACT

Rationale Alveolar epithelial cell apoptosis and protease/antiprotease imbalance based proteolysis play central roles in the pathogenesis of pulmonary emphysema but molecular mechanisms underlying these two events are not yet clearly understood. Cell adhesion molecule 1 (CADM1) is a lung epithelial cell adhesion molecule in the immunoglobulin superfamily. It generates two membrane associated C terminal fragments (CTFs), αCTF and βCTF, through protease mediated ectodomain shedding.

Objective To explore the hypothesis that more CADM1-CTFs are generated in emphysematous lungs through enhanced ectodomain shedding, and cause increased apoptosis of alveolar epithelial cells.

Methods and results Western blot analyses revealed that CADM1-CTFs increased in human emphysematous lungs in association with increased ectodomain shedding. Increased apoptosis of alveolar epithelial cells in emphysematous lungs was confirmed by terminal nucleotide nick end labelling (TUNEL) assays. NCI-H441 lung epithelial cells expressing mature CADM1 but not CTFs were induced to express αCTF both endogenously (by shedding inducers phorbol ester and trypsin) and exogenously (by transfection). Cell fractionation, immunofluorescence, mitochondrial membrane potentiometric JC-1 dye labelling and TUNEL assays revealed that CADM1-αCTF was localised to mitochondria where it decreased mitochondrial membrane potential and increased cell apoptosis. A mutation in the intracytoplasmic domain abrogated all three abilities of αCTF.

Conclusions CADM1 ectodomain shedding appeared to cause alveolar cell apoptosis in emphysematous lungs by producing αCTF that accumulated in mitochondria. These data link proteolysis to apoptosis, which are two landmark events in emphysema.

Key messages

What is the key question?

- Increased alveolar epithelial cell apoptosis and protease/antiprotease imbalance based proteolysis are two landmarks in the pathogenesis of pulmonary emphysema. What mechanisms may underlie these two events?

What is the bottom line?

- Lung epithelial cell adhesion molecule 1 (CADM1) generates two membrane associated C terminal fragments (CTFs), αCTF and βCTF, through protease mediated ectodomain shedding. CADM1-αCTF were increased in human emphysematous lungs, and appeared to cause alveolar epithelial cell apoptosis by localising to mitochondria and decreasing mitochondrial membrane potential.

Why read on?

- This study identifies CADM1-αCTF as a key molecule responsible for linking between proteolysis and apoptosis in emphysematous lungs, and will aid the development of a target based therapeutic strategy for emphysema.

INTRODUCTION

Emphysema is a pulmonary disease characterised by alveolar wall destruction, resulting in enlarged airspaces and loss of surface area for gas exchange without fibrosis.[1] This unique aspect of alveolar destruction has long been ascribed mainly to excessive apoptosis of alveolar structural (non-inflammatory) cells (ie, epithelial and endothelial cells), and a relative excess of proteases creating a local imbalance between proteases and antiproteases.[2 3] Apoptosis of endothelial cells in the alveolar wall is well explained by two mechanisms: decreased maintenance signals for endothelial cells mediated through vascular endothelial growth factor and its cognate receptor, and increased proteolysis of extracellular matrices in the alveolar wall resulting from a protease/antiprotease imbalance.[3 4] However, the molecular basis for alveolar epithelial cell apoptosis specific to emphysema is not yet fully understood. Involvement of a protease/antiprotease imbalance has generally been speculated because degradation of the extracellular matrix caused by excessive proteases forces alveolar cells to fall into anoikis, a type of programmed cell death, secondary to cell detachment from the matrix.[4] However, studies over the past decade have suggested that alveolar epithelial destruction in emphysematous lungs might occur due to apoptosis, possibly unrelated to matrix degradation induced by proteases. An in vitro experiment showed that leucocyte elastase induces apoptosis in lung epithelial cells by changing mitochondrial permeability, mediated by a protease activated receptor 1 triggered pathway

Open Access
Scan to access more free content

To cite: Mimae T, Hagiyama M, Inoue T, *et al*. *Thorax* 2014;**69**:223–231.

involving activation of nuclear factor κB and p53.[5] Cathepsin S, a cysteine proteinase secreted from pulmonary macrophages, mediates alveolar epithelial cell apoptosis in interferon γ induced emphysema of mice by activating both mitochondrial and death receptor pathways.[6] Matrix metalloproteinases trigger activation of the death receptor apoptotic pathway by processing the tumour necrosis factor α precursor and Fas ligand to yield their bioactive forms.[7 8] These results suggest that excessive proteases can directly act on alveolar epithelial cells and cause apoptosis, but this possibility has not been intensively examined.

Cell adhesion molecule 1 (CADM1), also widely known as tumour suppressor in lung cancer 1 (TSLC1), is an intercellular adhesion molecule in the immunoglobulin superfamily. It is a membrane spanning glycoprotein composed of three extracellular immunoglobulin-like domains, a single transmembrane region and a short carboxy terminal intracytoplasmic tail with a protein 4.1 interaction sequence and a PDZ type II domain binding motif.[9] CADM1 localises to the lateral plasma membrane in pulmonary and biliary epithelia and binds *trans*-homophilically between adjacent cells.[10 11] Consequently, it is assumed to contribute to the integrity of epithelial cell structure and polarity.[12] Recent studies by our own and other laboratories have revealed that CADM1 expression is regulated by post-transcriptional mechanisms, including glycosylation and proteolytic cleavage, called shedding.[13 14] CADM1 is cleaved at two sites in its ectodomain, yielding two membrane associated C terminal fragments (CTF), termed αCTF and βCTF. This ectodomain shedding appears to occur on the plasma membrane because this event proceeds in isolated plasma membranes and is directly mediated by a membrane bound metalloprotease called a disintegrin and metalloproteinase 10 (ADAM10).[14] These CTFs are subsequently cleaved within the plasma membrane by γ secretase, yielding an intracellular domain (ICD).[14] Although we previously proposed CADM1 shedding as a candidate mechanism for downregulating full length CADM1,[14] it remains unknown whether the products generated by shedding (ie, CTFs and ICD) have any biological function.

In the present study, we compared CADM1 expression between emphysematous and normal lungs and found that αCTF and βCTF increased in emphysematous lungs in association with increased ectodomain shedding of CADM1. Because alveolar cell apoptosis also increased in emphysematous lungs, we then examined the possible association between CADM1 ectodomain shedding and alveolar cell apoptosis. Human lung epithelial cells were induced to express endogenous αCTF by shedding inducers and were transfected to express exogenous αCTF. Cell fractionation and immunofluorescence experiments revealed that αCTF localised to mitochondria. This localisation appeared to result in mitochondrial depolarisation and induction of cell apoptosis. These data identify CADM1-αCTF as a key molecule that links two landmark events in emphysema, proteolysis and apoptosis.

MATERIALS AND METHODS

All materials and methods used in this study are described in detail in the online supplementary methods.

RESULTS

Increased shedding of CADM1 in emphysematous lungs

Surgically resected lungs were examined histologically by pathologists (see online supplementary figure S1), and 10 normal subjects and 11 patients with emphysematous lungs were enrolled. Patient characteristics are summarised in table 1. The histological diagnosis was consistent with the results of preoperative respiratory function tests, except that three subjects with normal lungs (case Nos 5, 8 and 9) had low carbon monoxide transfer factor (Tlco) and one patient with emphysematous lungs (case No 13) had fairly good forced expiratory volume at 1 s (FEV_1)/forced vital capacity (FVC) and Tlco. All patients with emphysematous lungs were cigarette smokers, as revealed by their Brinkman Indices (table 1). Based on this observation and our previous finding that smoking may alter CADM1 expression in the lung,[15] we subgrouped subjects with normal lungs into smokers (n=5) and non-smokers (n=5). The lung tissue lysates were analysed by western blotting with a polyclonal antibody raised against the CADM1 C terminal 15 amino acid peptide. CADM1 αCTF, βCTF and ICD were recognisable by this antibody. The full length form of CADM1 and its two shed forms, αCTF and βCTF, were detected at about 100, 20 and 35 kDa, respectively (figure 1A). Bands detected at 50 and 25 kDa corresponded to the non-glycosylated full length form and βCTF, respectively, as we reported previously.[11] The expression level of the full length form normalised to β-actin decreased significantly in emphysematous lungs compared with normal lungs (figure 1B). This might be attributable to a low content of epithelial cells in the tissue lysates because emphysematous lungs have a lower number of alveolar epithelial cells, the major source of CADM1 in the peripheral lung.[10] This speculation was supported by a western blot reprobed with an antibody against E-cadherin, an epithelial cell marker,[10] which revealed that the full length form of CADM1 and E-cadherin levels were well correlated in normal (R^2=0.734; p<0.001) and emphysematous (R^2=0.586; p<0.001) lungs (see online supplementary figure S2).

Table 1 Clinical characteristics of patients with normal and emphysematous lungs

	Normal (non-smoker)					Normal (smoker)					Emphysema (smoker)										
Case	1	2	3	4	5	6	7	8	9	10	11	12	13	14	15	16	17	18	19	20	21
Age (years)	64	50	48	63	76	60	56	80	71	84	79	62	62	68	76	58	80	70	70	84	79
Sex	F	M	M	F	F	M	F	M	M	M	M	M	M	M	M	F	F	M	M	M	M
Brinkman Index	0	0	0	0	0	900	500	2400	1000	2220	980	800	1600	1600	1000	600	200	1000	1000	1280	1200
Cause of surgery	AD	AD	AD	AD	AD	AD	AD	SCLC	SQ	AD	SQ	AD	AD	PC	AD	AD	AD	SCLC	CH	SQ	AD
Excised lung lobe*	RL	RU	RU	RU	LL	RU	RL	RU	RL	LU	RU	RU	RU	LU	LU	RU	RL	RU	RM	RU	RL
FEV_1/FVC	82.3	80.5	86.6	86.8	79.9	73.0	76.7	76.6	78.1	84.1	61.7	73.2	75.1	55.0	88.8	58.1	74.6	76.7	73.0	83.5	61.5
Tlco (%)	101.8	NE	92.8	76.5	49.3	102.0	81.2	57.0	41.2	89.3	37.8	NE	71.2	NE	44.4	36.8	55.3	54.8	53.0	36.3	68.2

AD, adenocarcinoma; CH, chondroid hamartoma; FEV_1, forced expiratory volume in 1 s; FVC, forced vital capacity; NE, not examined; PC, plemorphic carcinoma; SCLC, small cell lung carcinoma; SQ, squamous cell carcinoma; Tlco, carbon monoxide transfer factor.
*LL, left lower; LU, left upper; RL, right lower; RM, right middle; RU, right upper.

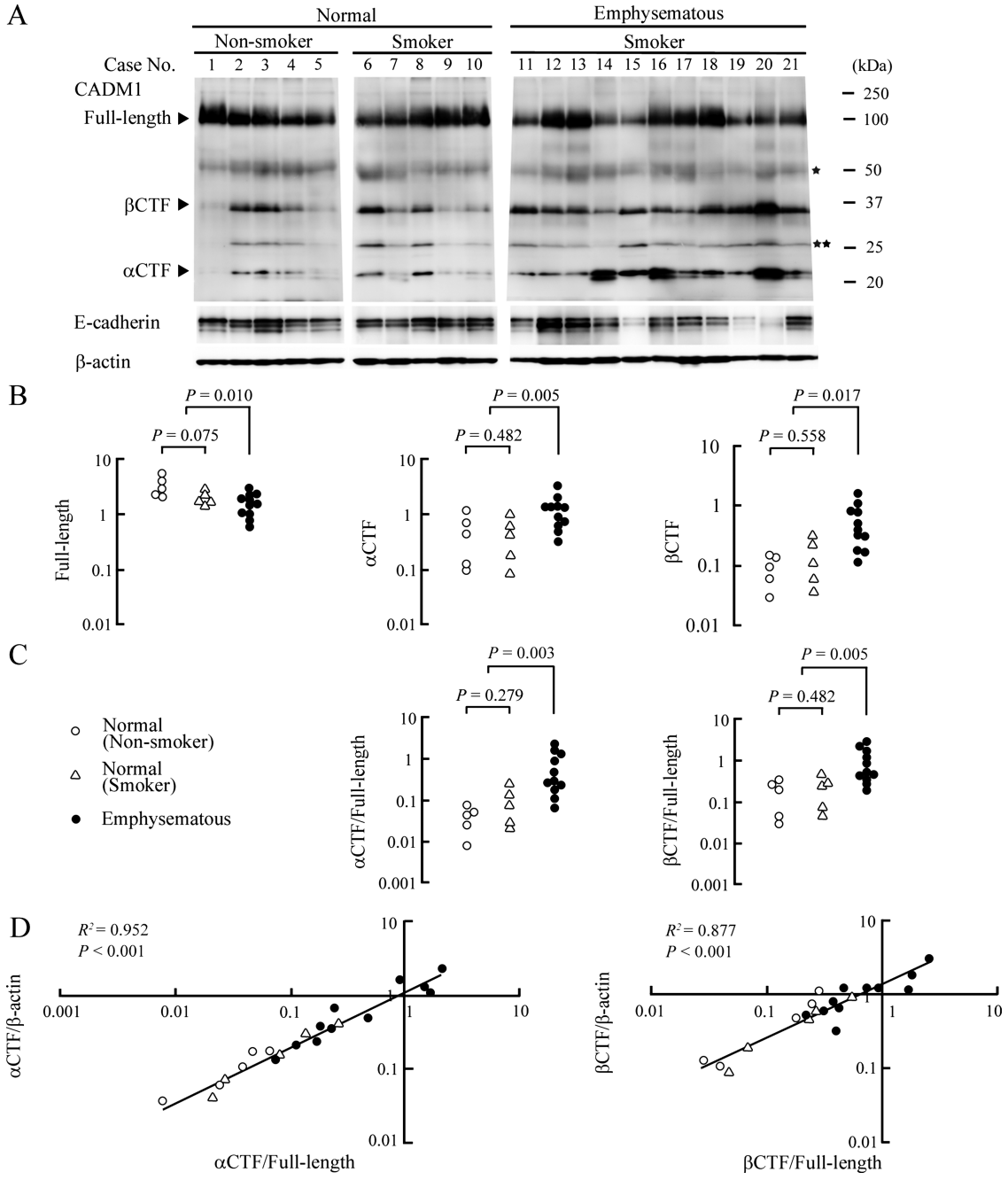

Figure 1 Increased ectodomain shedding of cell adhesion molecule 1 (CADM1) in emphysematous lungs. (A) Western blot analyses of CADM1 and E-cadherin in normal and emphysematous lungs. Cases are numbered as in table 1. Bands corresponding to the non-glycosylated full length form and β C terminal fragment (CTF) are depicted by one and two asterisks, respectively. The blots were reprobed with an anti-β-actin antibody to indicate protein loading per lane. (B) Graphs plotted with dots indicating relative expression levels of CADM1 molecules. In each lane of (A), intensities of bands specific to CADM1 full length form, αCTF and βCTF, and β-actin were quantified using NIH ImageJ software, and the intensities of CADM1 molecules were normalised to β-actin. Statistical significance was analysed by the Mann–Whitney U test, and p values are shown. (C) Graphs plotted with dots indicating expression levels of αCTF and βCTF relative to the full length form of CADM1. Statistical significance was analysed by the Mann–Whitney U test, and p values are shown. (D) Graphs with X and Y axes in band intensity ratios. On the left, αCTF/full length and αCTF/β-actin were plotted on the X and Y axes, respectively. On the right, βCTF/full length and βCTF/β-actin were plotted on the X and Y axes, respectively. In each graph, the two ratios were well approximated as linear. Correlations and statistical significance were analysed by Spearman's rank test, and R^2 and p values are shown.

In contrast, expression levels of αCTF and βCTF increased significantly in emphysematous lungs, while they were comparable between smokers and non-smokers with normal lungs (figure 1B). We also calculated the signal intensity ratios of αCTF and βCTF to the full length form for each case, and found that these ratios were significantly higher in emphysematous lungs than those in normal lungs (figure 1C), and were strongly positively correlated with αCTF and βCTF levels (R^2=0.952 and 0.877; p<0.001), respectively (figure 1D). The ratios of the two shed forms were comparable between smokers and non-smokers with normal lungs. These results indicate that CADM1 ectodomain shedding was

accelerated to generate more αCTF and βCTF in emphysematous lungs.

Increased apoptosis of alveolar cells in emphysematous lungs

Lung sections were double stained by the terminal deoxynucleotidyl transferase mediated dUTP nick end labelling (TUNEL; green) and E-cadherin immunofluorescence (red) (figure 2A, B). Alveolar epithelial cells were identified by membranous staining for E-cadherin. Practically all alveolar cells were TUNEL negative in normal lungs, irrespective of smoking habit, whereas >10% of alveolar cells on average were TUNEL positive in emphysematous lungs ($p<0.002$) (figure 2C).

CADM1-αCTF localises to mitochondria

To probe for a possible link between increased CADM1 ectodomain shedding and increased alveolar cell apoptosis, we used NCI-H441 cells, a human lung epithelial cell line with characteristics of Clara cells. Western blot analyses detected abundant expression of the full length form of CADM1 in NCI-H441 cells grown under standard culture conditions, but the two shed forms αCTF and βCTF were undetectable, indicating that CADM1 was rarely shed in steady state NCI-H441 cells. We used phorbol 12-myristate 13-acetate (PMA) and trypsin to induce CADM1 shedding, which both induce ectodomain shedding of transmembrane proteins.[14 16] When the cells were treated with a mixture of PMA (200 nM) and trypsin (0.0125% w/v, a concentration low enough to prevent cell detachment) for 20 min, but not with either alone, a considerable amount of αCTF appeared with a slight decrease in the amount of full length CADM1, indicating that CADM1 ectodomain shedding was induced by the treatment (figure 3). The reason why βCTF was not produced by the treatment is unknown. Considering that β shedding of β-amyloid precursor protein, a key event in Alzheimer's disease, occurs within cells,[17] trypsin may have no potential to activate β shedding due to its inaccessibility to β-sheddase(s).

PMA and trypsin treated or untreated cells were then double stained by CADM1 immunofluorescence and Mitotracker dye, a mitochondrial marker. CADM1 immunostaining was exclusively

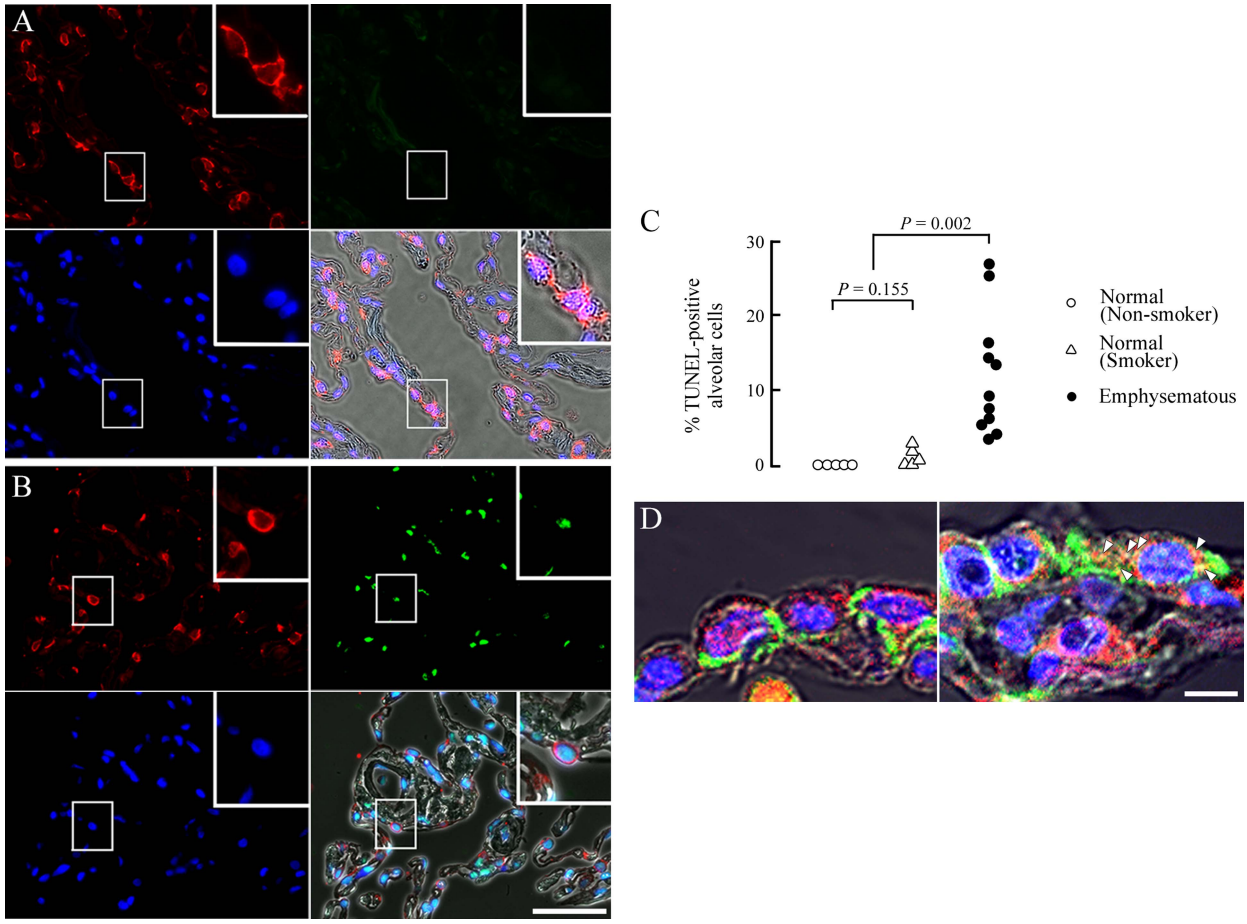

Figure 2 Increased apoptosis of alveolar epithelial cells in emphysematous lungs. (A, B) Representative results of terminal deoxynucleotidyl transferase dUTP nick end labelling (TUNEL) assays for normal (A) and emphysematous (B) lungs. Formalin fixed, paraffin embedded lung sections were triple stained by E-cadherin immunofluorescence (red; left upper), the TUNEL method (green; right upper) and 4′,6-diamino-2-phenylindole (DAPI, for nuclear counterstain; blue; left lower). These three images were merged on the differential interference contrast image (right lower). TUNEL negative and positive alveolar epithelial cells are enlarged in insets of (A) and (B), respectively. Bar=50 μm. (C) Graph plotted with dots indicating TUNEL positive alveolar epithelial cell proportions in individual patients who were divided into two groups, normal and emphysematous lungs. The normal lung patients were further divided into non-smokers and smokers. Statistical significance was analysed between groups by the Student's t test, and p values are shown. (D) Double immunofluorescence of normal (left) and emphysematous (right) lung sections for cell adhesion molecule 1 (CADM1) (green) and mitochondria (clone 113–1; red). Sections were counterstained by DAPI (blue). Three fluorescence images are merged on the differential interference contrast image. Arrowheads point to examples of colocalisation of CADM1 and mitochondrial immunostaining. Bar=10 μm.

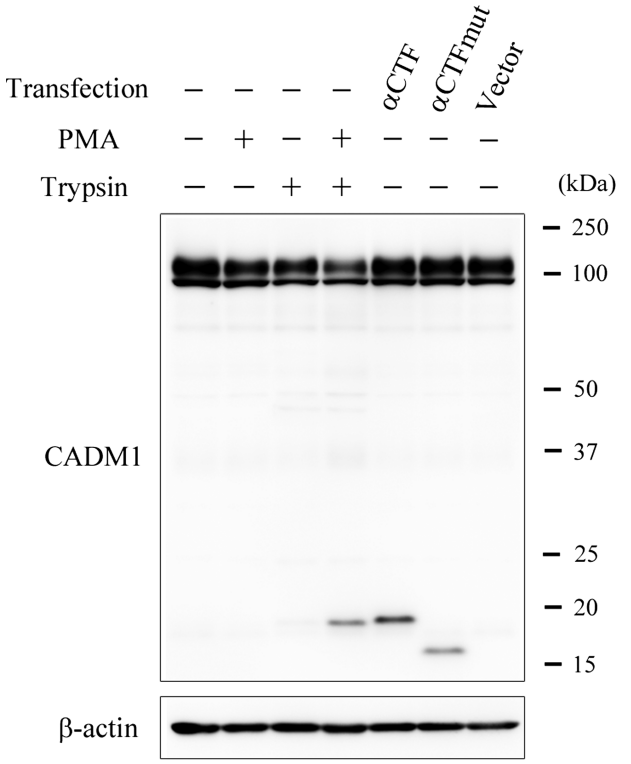

Figure 3 Induction of cell adhesion molecule 1 (CADM1) ectodomain shedding and exogenous expression of α C terminal fragment (CTF) and αCTFmut in NCI-H441 cells. NCI-H441 cells were treated with either phorbol myristic acid (PMA 200 nM) or trypsin (0.0125% w/v), or a mixture of both, or were transfected with pCX4bsr-SP-αCTF, pCX4bsr-SP-αCTFmut or an empty vector. After 20 min of treatment and 2 days of transfection, the cells were subjected to western blot analyses with the CADM1 antibody.

detected on the cell membrane of untreated cells (figure 4Aa), whereas PMA and trypsin treatment resulted in a marked appearance of cytoplasmic stains for CADM1, which were significantly colocalised with Mitotracker stain (figure 4Ab, B), suggesting subcellular localisation of CADM1-αCTF to mitochondria.

We examined this possibility by expressing αCTF exogenously. Because CADM1 ectodomain shedding likely occurs on the cell surface,[14] αCTF should be primarily a transmembrane protein. Thus according to our previous mass spectrometric data that determined the N terminal amino acid residue of αCTF,[14] we constructed a plasmid vector expressing a large deletion form of CADM1, in which the signal peptide was ligated upstream of αCTF (pCX4bsr-SP-αCTF). We mutated the intracytoplasmic domain of αCTF as a control so that the resulting domain would not target to mitochondria but to the cytosol (pCX4bsr-SP-αCTFmut; online supplementary figure S3), according to an intracellular localisation prediction algorithm (WoLF PSORT; refer to online supplementary methods). We transfected NCI-H441 cells with either plasmid construct, and 2 days later confirmed that the transfectants expressed a considerable amount of exogenous αCTF or αCTFmut by western blot analyses (figure 3). The ratios of αCTF to full length CADM1 in transfectants were equivalent to those in emphysematous lungs (see online supplementary figure S4). Taken together with the western blot results indicating that endogenous full length CADM1 in NCI-H441 cells was certainly lower than that in normal lung epithelial cells in vivo (see online supplementary figure S4), transfectants with pCX4bsr-SP-αCTF were considered to resemble epithelial cells from emphysematous lungs rather than normal lungs, in terms of CADM1 protein levels.

NCI-H441 transfectants were double stained with CADM1 immunofluorescence and Mitotracker dye. Transfectants with pCX4bsr-SP-αCTF exhibited a staining pattern quite similar to that of PMA and trypsin treated cells; the cytoplasmic CADM1 signals were well colocalised with Mitotracker stain (figure 4Ac, B). In contrast, pCX4bsr-SP-αCTFmut transfectants showed a strong CADM1 membranous staining with weak but significant cytoplasmic signals that were rarely colocalised with Mitotracker stain (figure 4Ad, B).

Mitochondrial localisation of αCTF was examined by cell fractionation of NCI-H441 cells expressing endogenous and exogenous αCTF. Exogenous αCTF and αCTFmut were expressed as N terminally FLAG tagged forms to clearly distinguish them from endogenous αCTF using the p3xFLAG-CMV-9 vector, which is designed to deliver the protein encoded by the cDNA insert efficiently to the cell surface. Expression of FLAG tagged proteins was confirmed by western blotting with an anti-FLAG antibody (see online supplementary figure S5). Transfected or untransfected NCI-H441 cells were treated with a mixture of PMA (200 nM) and trypsin (0.25% w/v) for 20 min to induce endogenous αCTF and detach cells without mitochondrial damage and then were fractionated into cytosolic and mitochondrial fractions. Whole cytoplasmic lysates without nuclei were also prepared from aliquots of the treated cells. Successful fractionation was verified by western blotting analyses, showing enrichment of glyceraldehyde 3-phosphate dehydrogenase (G3PDH), a cytosolic marker, and cytochrome c oxidase subunit IV (CoxIV), a mitochondrial marker, in the corresponding fractions (figure 5). Reprobing with the CADM1 antibody revealed that both endogenous and exogenous αCTFs were detected exclusively in the mitochondrial fraction as CoxIV, whereas αCTFmut was enriched in the cytosolic fraction as greatly as G3PDH (figure 5).

Lung sections were double stained with antibodies against CADM1 and mitochondria. CADM1 immunostaining in alveolar epithelial cells was primarily membranous in normal lungs whereas it was occasionally both membranous and cytoplasmic in emphysematous lungs and cytoplasmic staining was appreciably colocalised with mitochondrial staining (figure 2D). The proportion of epithelial cells with this colocalisation signal was significantly larger in emphysematous lungs (n=4) than in normal lungs (n=4) (11.3±8.3 vs 1.8±1.5%; p=0.038).

CADM1-αCTF decreases mitochondrial membrane potential and induces apoptosis

We examined whether CADM1-αCTF might alter mitochondrial membrane potential (ΔΨm) that normally exists across the inner mitochondrial membrane using the JC-1 probe, a lipophilic cationic dye that exhibits ΔΨm dependent accumulation in mitochondria, as indicated by a fluorescence shift from green (~525 nm) to red (~590 nm). NCI-H441 transfectants expressing exogenous αCTF or αCTFmut were stained with JC-1 dye at 24, 48 and 72 h post-transfection, and mitochondrial depolarisation was assessed by measuring the red/green fluorescence intensity ratio of the dye (figure 6A and see online supplementary figure S6). αCTFmut did not change the JC-1 ratio at any time point, whereas αCTF significantly decreased the ratio at 48 and 72 h (figure 6B). Transfected and untransfected NCI-H441 cells were stained by the TUNEL technique 48 h after transfection. αCTFmut did not change the proportion

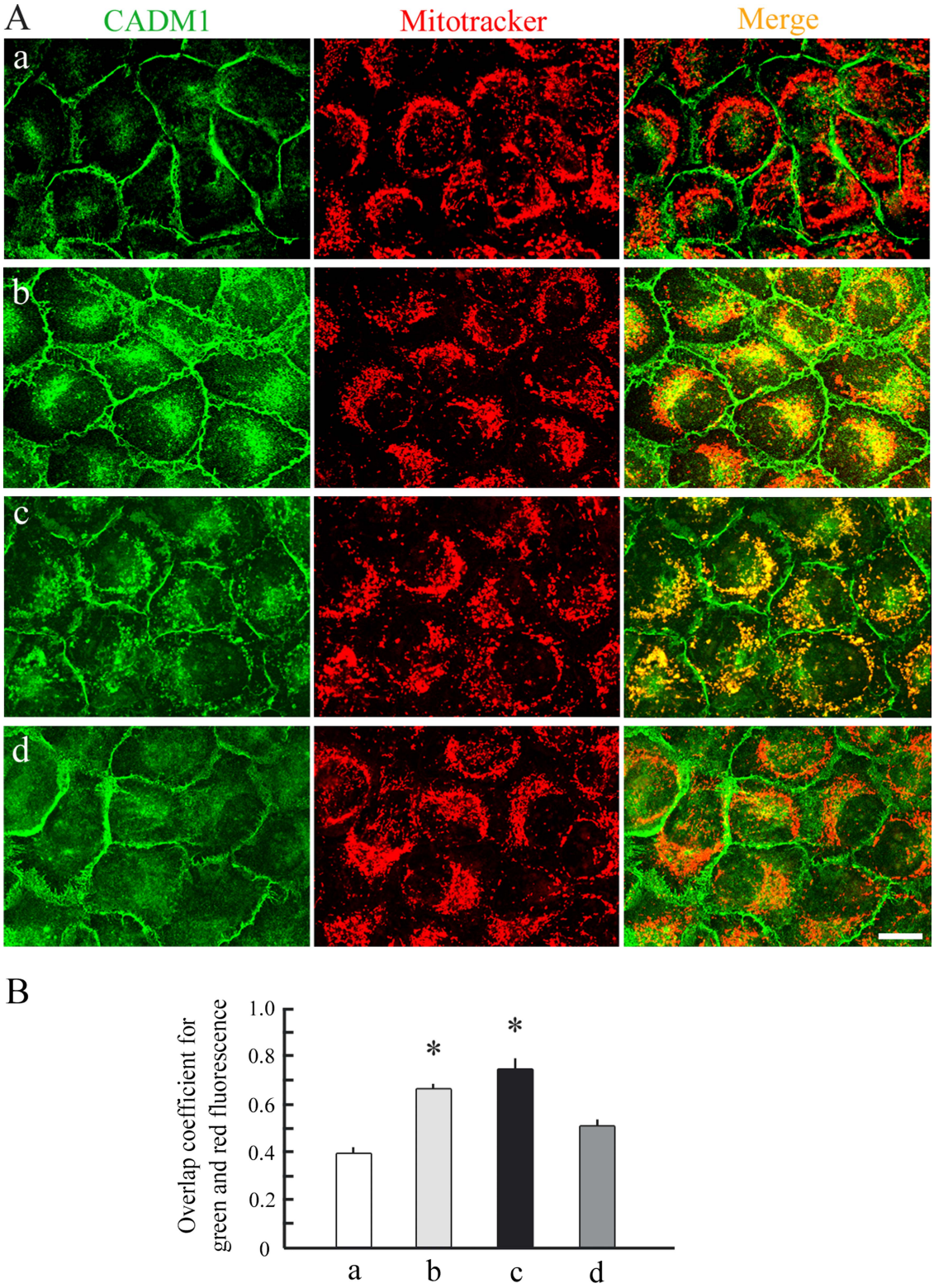

Figure 4 Immunofluorescence of cell adhesion molecule 1 (CADM1) with Mitotracker staining in NCI-H441 cells expressing α C terminal fragment (CTF) and αCTFmut. (A) NCI-H441 cells were untreated (a) or treated with a mixture of phorbol myristic acid and trypsin (b), or were transfected with pCX4bsr-SP-αCTF (c) or pCX4bsr-SP-αCTFmut (d). Then, cells were double stained with CADM1 immunofluorescence (green; left) and Mitotracker fluorescence (red; middle). In the merged images (right), yellow areas mean colocalisation of both fluorescent signals—that is, mitochondrial localisation of CADM1. Bar=10 μm. (B) Graph showing overlap coefficients in NCI-H441 cells of the four types (a–d shown in (A)). Intensity correlation between green and red fluorescence was quantified using ImageJ Colocalisation Analysis, and overlap coefficients were calculated. Data are expressed as mean±SD, and statistical significance was analysed by the Student's t test. *p<0.01 compared with the value of untreated cells (a in (A)).

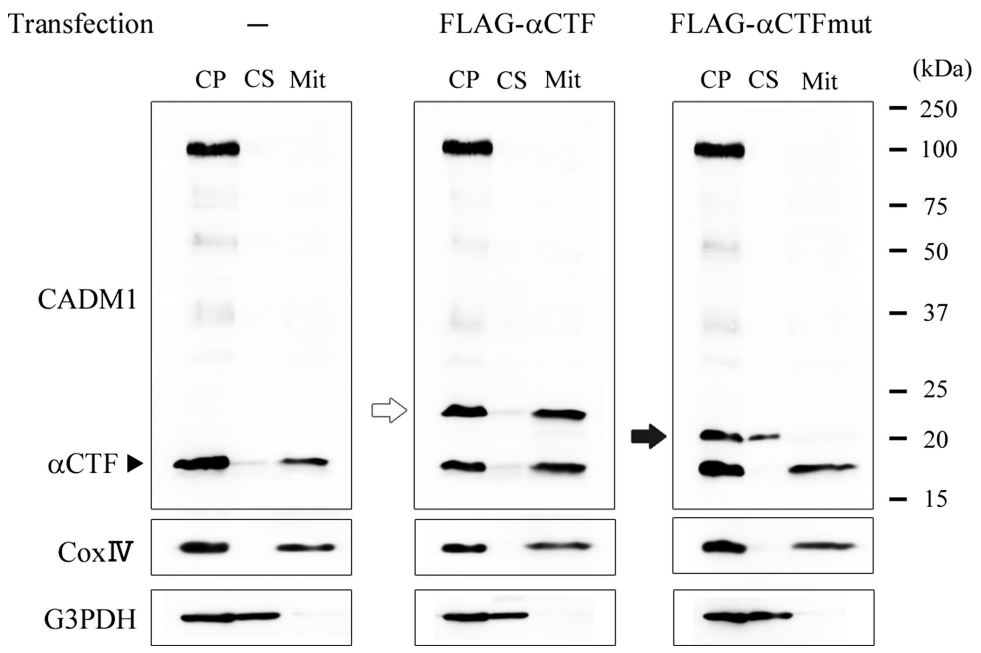

Figure 5 Cell fractionation experiments of NCI-H441 cells expressing α C terminal fragment (CTF) and αCTFmut. NCI-H441 cells were untransfected (left) or transfected with p3xFLAG-αCTF (middle) or p3xFLAG-αCTFmut (right), and were fractionated into cytosolic (CS) and mitochondrial (Mit) fractions. Whole cytoplasmic lysates (CP) were extracted from aliquots of the cells. These lysates and fractions were analysed with western blotting using antibodies against cell adhesion molecule 1 (CADM1), cytochrome c oxidase subunit IV (CoxIV) and glyceraldehyde 3-phosphate dehydrogenase (G3PDH). Open and closed arrows indicate FLAG tagged αCTF and αCTFmut, respectively.

of TUNEL positive cells whereas αCTF increased the proportion fivefold ($p<0.01$) (figure 6B).

DISCUSSION

We found that CADM1 ectodomain shedding increased in emphysematous lungs from smoking patients, but not in normal lungs from smoking patients, suggesting that oxidants in cigarette smoke may act as a critical inducer of CADM1 ectodomain shedding only in subjects who have particular genetic backgrounds. Of interest, changes in emphysema susceptible genes, such as α-1 antitrypsin,[18] macrophage elastase,[19] klotho[20] and surfactant D,[21] lead to a relative excess of proteases, creating a local protease/antiprotease imbalance.[19 21–23] In the present study, all patients with smoking habits were obliged to quit smoking more than 1 month before the date of surgery. Therefore, oxidants seem not to promote CADM1 shedding through its direct ongoing action but rather seem to help establish long lasting protease/antiprotease imbalances in alveoli.

All but one patient (case No 19) analysed in this study had lung cancer. Because CADM1 is known to be downregulated in lung cancer due to promoter methylation,[24] these patients had potentially impaired CADM1 expression even in non-cancerous lungs. We performed western blot analyses of a small number of emphysematous lungs that did not develop lung cancer, and detected a relative increase in αCTF and βCTF to full length CADM1 (see online supplementary figure S7). Increased amounts of αCTF and βCTF appeared to be present in emphysematous lungs as a result of increased ectodomain shedding of CADM1 in emphysematous lungs, both with and without lung cancer.

Cell fractionation and immunofluorescence experiments consistently showed that αCTF localised to mitochondria. This finding appeared to be relevant in vivo, as we detected intracytoplasmic CADM1 that was associated with mitochondria in alveolar epithelial cells from emphysematous lungs (figure 2D). Mutagenesis experiments revealed a decisive role for the intracytoplasmic domain in this subcellular localisation. How the intracytoplasmic domain leads αCTF to mitochondria remains to be addressed. A growing body of evidence is accumulating to show that cell membrane spanning proteins, such as epidermal growth factor receptor and mucin 1, can translocate to mitochondria.[25 26] Although mechanisms underlying these events remain largely unknown, clathrin mediated endocytosis is shown to be involved.[26] After internalisation, mucin 1 is assumed to utilise heat shock proteins as molecular chaperons for mitochondrial translocation.[25] Higashiyama *et al* demonstrated that the remnant peptides generated by ectodomain shedding of type I integral membrane proteins, such as pro-heparin binding epidermal growth factor-like growth factor and pro-amphiregulin, are internalised into endocytotic vesicles.[27 28] The N and C termini of the peptides are positioned inside and outside of the vesicles, respectively, and the C terminal tail, free in the cytosol, plays a decisive role in the intracellular destinations of the remnant peptide.[27 28] αCTF may be present as a vesicle associated transmembrane molecule in the cytoplasm, with its C terminal tail being free outside the vesicle, and this C terminal tail may carry a conformational signal that serves as a binding site for molecular chaperons, such as heat shock protein family members.

Exogenous αCTF decreased mitochondrial membrane potential in NCI-H441 cells and increased apoptosis, suggesting that mitochondrial localisation of αCTF might result in activation of the mitochondrial apoptosis pathway. Mao *et al* reported that exogenous CADM1 induces caspase 3 activation and apoptosis in A549 lung adenocarcinoma cells lacking endogenous CADM1, and that protein 4.1 binding motif and PDZ domain binding motif in the intracytoplasmic domain are indispensable for this induction.[29] Members of the membrane associated guanylate kinase (MAGuK) family are known as binding partners to the latter motif.[30] Interestingly, this family contains a subgroup that carries the caspase recruitment domain in its N terminal

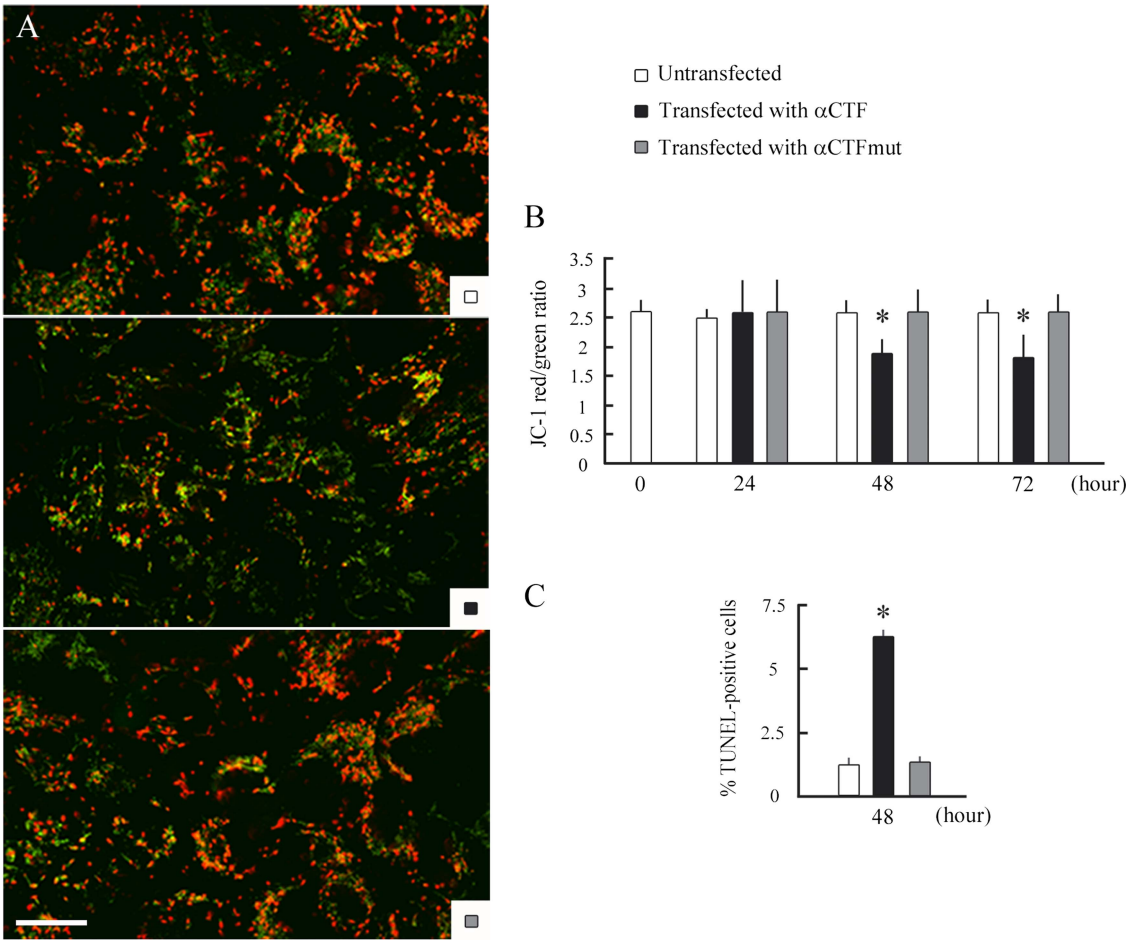

Figure 6 α C terminal fragment (CTF) decreases mitochondrial membrane potential in NCI-H441 cells and increases apoptosis. (A) Representative results of JC-1 staining in NCI-H441 cells. NCI-H441 cells were untransfected (upper) or transfected with pCX4bsr-SP-αCTF (middle) or pCX4bsr-SP-αCTFmut (lower), and were stained 48 h later with JC-1 dye. Images were captured by a confocal laser microscope, and green and red fluorescence signals were merged. Differential interference contrast images are shown in online supplementary figure S6. Bar=20 μm. (B) Graph showing changes in JC-1 red/green ratios in NCI-H441 cells after transfection. NCI-H441 cells were untransfected or transfected with pCX4bsr-SP-αCTF or pCX4bsr-SP-αCTFmut, and were stained with JC-1 dye at the indicated time points. Cells were observed through a confocal laser microscope and were morphometrically analysed to calculate JC-1 red/green ratios. Data are expressed as mean± SD, and statistical significance was analysed by the Student's t test. *p<0.01 compared with the value of untransfected cells. (C) Graph showing the proportion of terminal deoxynucleotidyl transferase dUTP nick end labelling (TUNEL) positive NCI-H441 cells at 2 days after transfection. Cells were transfected as in (B). After 2 days, cells were stained with the TUNEL method, and the proportions of TUNEL positive cells were calculated. Data are expressed as mean±SD, and statistical significance was analysed by the Mann–Whitney U test. *p<0.01 compared with the value in untransfected cells.

region and participates in apoptosis signalling.[31] αCTF and βCTF, which both share the intracytoplasmic domain, once produced, may activate the mitochondrial apoptosis pathway by transporting particular MAGuK family members to mitochondria in alveolar epithelial cells.

There are several splice variants of human CADM1, named isoforms SP1 to SP4.[32] Reverse transcription-PCR revealed that nine lungs examined and NCI-H441 cells all expressed SP4 exclusively (see online supplementary figure S8). Tanabe *et al* showed that SP1 and SP2 are shed constitutively, while SP3 is non-cleavable.[33] Our data proved SP4 cleavable. SP4 ectodomain shedding appeared to be not constitutive but induced by particular pathological stimuli. Moiseeva *et al* reported that SP4 overexpressing HMC-1 mast cells show better survival and lower caspase 3/7 activity than SP1 overexpressing cells.[34] This difference between two isoforms may be explained by their distinct susceptibility to ectodomain shedding. In HMC-1 cells, SP1 may produce more αCTF and/or βCTF than SP4, resulting in activation of the mitochondrial apoptosis pathway.

In conclusion, we propose increased ectodomain shedding of CADM1 as a novel molecular mechanism for increased alveolar cell apoptosis in emphysematous lungs. This mechanism is an extension of the conventional understanding that proteolytic activity is locally excessive in emphysematous lung alveoli because CADM1 ectodomain shedding per se is a proteolytic process, and also suggests that selective inhibitors to block CADM1 sheddase activity and/or mitochondrial localisation of CADM1 shedding products can slow or halt the progression of emphysema. In fact, ADAM10 is released by human alveolar macrophages, and intratracheal administration of an adenoviral vector expressing ADAM10 in mice results in the development of emphysema.[35] Further characterisation of CADM1 ectodomain shedding and its associated molecular events will open a new avenue for target based therapeutic approaches to emphysema.

Contributors AI and YM designed the study, and AI wrote the manuscript. AI, TM and MO provided the clinical samples. TM, MH, TI, AY and TK performed the experiments, and MH analysed the data.

Funding This study was supported by the Japan Society for the Promotion of Science Kakenhi (24890274 and 25860302 to MH, 24659184 to TI, 24890137 to TM, and 24590492 to AI), and grants from the Yasuda Medical Foundation and the Osaka Medical Research Foundation for Intractable Diseases.

Competing interests None.

Patient consent Obtained.

Ethics approval Ethics approval was provided by the ethics committee of Hiroshima University and Kinki University, Japan (approval Nos Eki-350 and 25–088).

Provenance and peer review Not commissioned; externally peer reviewed.

REFERENCES

1 Snider GL, Kleinerman J, Thurlbeck WM, *et al*. The definition of emphysema. Report of a National Heart, Lung, and Blood Institute, Division of Lung Diseases workshop. *Am Rev Respir Dis* 1985;132:182–85.
2 Tuder RM, Petrache I, Elias JA, *et al*. Apoptosis and emphysema: the missing link. *Am J Respir Cell Mol Biol* 2003;28:551–4.
3 Taraseviciene-Stewart L, Voelkel NF. Molecular pathogenesis of emphysema. *J Clin Invest* 2008;118:394–402.
4 Demedts IK, Demoor T, Bracke KR, *et al*. Role of apoptosis in the pathogenesis of COPD and pulmonary emphysema. *Respir Res* 2006;7:53.
5 Suzuki T, Yamashita C, Zemans RL, *et al*. Leukocyte elastase induces lung epithelial apoptosis via a PAR-1-, NF-kappaB-, and p53-dependent pathway. *Am J Respir Cell Mol Biol* 2009;41:742–55.
6 Zheng T, Kang MJ, Crothers K, *et al*. Role of cathepsin S-dependent epithelial cell apoptosis in IFN-gamma-induced alveolar remodeling and pulmonary emphysema. *J Immunol* 2005;174:8106–15.
7 Powell WC, Fingleton B, Wilson CL, *et al*. The metalloproteinase matrilysin proteolytically generates active soluble Fas ligand and potentiates epithelial cell apoptosis. *Curr Biol* 1999;9:1441–7.
8 Mohan MJ, Seaton T, Mitchell J, *et al*. The tumor necrosis factor-alpha converting enzyme (TACE): a unique metalloproteinase with highly defined substrate selectivity. *Biochemistry* 2002;41:9462–9.
9 Kuramochi M, Fukuhara H, Nobukuni T, *et al*. TSLC1 is a tumor-suppressor gene in human non-small-cell lung cancer. *Nat Genet* 2001;27:427–30.
10 Ito A, Okada M, Uchino K, *et al*. Expression of the TSLC1 adhesion molecule in pulmonary epithelium and its down-regulation in pulmonary adenocarcinoma other than bronchioloalveolar carcinoma. *Lab Invest* 2003;83:1175–83.
11 Ito A, Nishikawa Y, Ohnuma K, *et al*. SgIGSF is a novel biliary-epithelial cell adhesion molecule mediating duct/ductule development. *Hepatology* 2007;45:684–94.
12 Sakurai-Yageta M, Masuda M, Tsuboi Y, *et al*. Tumor suppressor CADM1 is involved in epithelial cell structure. *Biochem Biophys Res Commun* 2009;390:977–82.
13 Fogel AI, Li Y, Giza J, *et al*. N-glycosylation at the SynCAM (synaptic cell adhesion molecule) immunoglobulin interface modulates synaptic adhesion. *J Biol Chem* 2010;285:34864–74.
14 Nagara Y, Hagiyama M, Hatano N, *et al*. Tumor suppressor cell adhesion molecule 1 (CADM1) is cleaved by a disintegrin and metalloprotease 10 (ADAM10) and subsequently cleaved by gamma-secretase complex. *Biochem Biophys Res Commun* 2012;417:462–7.
15 Kikuchi S, Yamada D, Fukami T, *et al*. Hypermethylation of the TSLC1/IGSF4 promoter is associated with tobacco smoking and a poor prognosis in primary nonsmall cell lung carcinoma. *Cancer* 2006;106:1751–8.
16 Ding K, Lopez-Burks M, Sanchez-Duran JA, *et al*. Growth factor-induced shedding of syndecan-1 confers glypican-1 dependence on mitogenic responses of cancer cells. *J Cell Biol* 2005;171:729–38.
17 Chyung AS, Greenberg BD, Cook DG, *et al*. Novel beta-secretase cleavage of beta-amyloid precursor protein in the endoplasmic reticulum/intermediate compartment of NT2N cells. *J Cell Biol* 1997;138:671–80.
18 Martorana PA, Brand T, Gardi C, *et al*. The pallid mouse. A model of genetic alpha 1-antitrypsin deficiency. *Lab Invest* 1993;68:233–41.
19 Hautamaki RD, Kobayashi DK, Senior RM, *et al*. Requirement for macrophage elastase for cigarette smoke-induced emphysema in mice. *Science* 1997;277:2002–4.
20 Kuro-o M, Matsumura Y, Aizawa H, *et al*. Mutation of the mouse klotho gene leads to a syndrome resembling ageing. *Nature* 1997;390:45–51.
21 Wert SE, Yoshida M, LeVine AM, *et al*. Increased metalloproteinase activity, oxidant production, and emphysema in surfactant protein D gene-inactivated mice. *Proc Natl Acad Sci U S A* 2000;97:5972–7.
22 Kidokoro Y, Kravis TC, Moser KM, *et al*. Relationship of leukocyte elastase concentration to severity of emphysema in homozygous alpha1-antitrypsin-deficient persons. *Am Rev Respir Dis* 1977;115:793–803.
23 Funada Y, Nishimura Y, Yokoyama M. Imbalance of matrix metalloproteinase-9 and tissue inhibitor of matrix metalloproteinase-1 is associated with pulmonary emphysema in Klotho mice. *Kobe J Med Sci* 2004;50:59–67.
24 Fukami T, Fukuhara H, Kuramochi M, *et al*. Promoter methylation of the TSLC1 gene in advanced lung tumors and various cancer cell lines. *Int J Cancer* 2003;107:53–9.
25 Ren J, Bharti A, Raina D, *et al*. MUC1 oncoprotein is targeted to mitochondria by heregulin-induced activation of c-Src and the molecular chaperone HSP90. *Oncogene* 2006;25:20–31.
26 Demory ML, Boerner JL, Davidson R, *et al*. Epidermal growth factor receptor translocation to the mitochondria: regulation and effect. *J Biol Chem* 2009;284:36592–604.
27 Hieda M, Isokane M, Koizumi M, *et al*. Membrane-anchored growth factor, HB-EGF, on the cell surface targeted to the inner nuclear membrane. *J Cell Biol* 2008;180:763–9.
28 Isokane M, Hieda M, Hirakawa S, *et al*. Plasma-membrane-anchored growth factor pro-amphiregulin binds A-type lamin and regulates global transcription. *J Cell Sci* 2008;121:3608–18.
29 Mao X, Seidlitz E, Truant R, *et al*. Re-expression of TSLC1 in a non-small-cell lung cancer cell line induces apoptosis and inhibits tumor growth. *Oncogene* 2004;23:5632–42.
30 Murakami Y. Involvement of a cell adhesion molecule, TSLC1/IGSF4, in human oncogenesis. *Cancer Sci* 2005;96:543–52.
31 Bertin J, Wang L, Guo Y, *et al*. CARD11 and CARD14 are novel caspase recruitment domain (CARD)/membrane-associated guanylate kinase (MAGUK) family members that interact with BCL10 and activate NF-kappa B. *J Biol Chem* 2001;276:11877–82.
32 Biederer T. Bioinformatic characterization of the SynCAM family of immunoglobulin-like domain-containing adhesion molecules. *Genomics* 2006;87:139–50.
33 Tanabe Y, Kasahara T, Momoi T, *et al*. Neuronal RA175/SynCAM1 isoforms are processed by tumor necrosis factor-alpha-converting enzyme (TACE)/ADAM17-like proteases. *Neurosci Lett* 2008;444:16–21.
34 Moiseeva EP, Leyland ML, Bradding P. CADM1 is expressed as multiple alternatively spliced functional and dysfunctional isoforms in human mast cells. *Cell Mol Life Sci* 2012;69:2751–64.
35 Saitoh H, Leopold PL, Harvey BG, *et al*. Emphysema mediated by lung overexpression of ADAM10. *Clin Transl Sci* 2009;2:50–6.

Online data supplement to:

Revised manuscript thoraxjnl-2013-203867.R1

Original Article

Increased ectodomain shedding of lung-epithelial cell adhesion molecule 1 as a cause of increased alveolar cell apoptosis in emphysema

Table of Contents

Supplementary methods (pages 2-11)

Figure legends for supplementary figures S1-S8 (pages 12-15)

Supplementary methods

Antibodies and reagents

A rabbit anti-CADM1 polyclonal antibody directed against the C-terminal 15-amino acid peptide was generated in our laboratory and described previously.[1] CADM1 αCTF, βCTF and ICD were recognizable by this antibody (Supplementary figure S3). Other primary antibodies used were against E-cadherin (clone 36; BD Bioscience, San Jose, CA, USA), FLAG (M2; Sigma-Aldrich, St. Louis, MO, USA), CoxIV (3E11; Cell Signalling Technology, Danvers, MA, USA), G3PDH (Merck Millipore, Billerica, MA, USA), and mitochondria (clone 113-1 recognizing a ~60-kDa mitochondrial protein; Merck Millipore). Peroxidase- and fluorophore-conjugated secondary antibodies were obtained from Amersham (Bukinghamshine, England) and Jackson ImmunoResearch (West Grove, PA, USA), respectively. PMA and trypsin were purchased from Wako Pure Chemical Industries (Osaka, Japan).

Cell culture

NCI-H441 human lung epithelial cells were purchased from the American Type Culture Collection (Rockville, MD, USA) in 2010 (Lot No. 58294188), and all experimentation using this cell line proceeded within 6 months after resuscitation. NCI-H441 cells were grown in Roswell Park Memorial Institute medium (RPMI-1640; Nacalai Tesque, Kyoto, Japan) supplemented with 10% fetal bovine serum (FBS), antibiotics containing 100 units/mL penicillin and 100 μg/mL streptomycin (Invitrogen, Carlsbad, CA, USA), and 5 mM HEPES buffer (Sigma-Aldrich) at 37°C in 5% CO_2/95% air. To induce CADM1 ectodomain shedding, NCI-H441 cells were incubated in RPMI-1640 medium containing 200 nM PMA, 0.0125% w/v trypsin (a concentration low enough to prevent

cell detachment), or a mixture of both, for 20 min. Lung cancer cell lines A549 and NCI-H596 were described previously.[2]

Human samples

Human lung tissues were obtained from patients who were diagnosed with lung cancer or tumourous masses and underwent pulmonary lobectomy or segmentectomy at Hiroshima University Hospital (Hiroshima, Japan) between 2008 and 2012. All patients with a smoking habit were obliged to quit smoking more than 1 month before the date of surgery. Immediately after the operation, non-cancerous portions (approximately 2 cm^3) of the surgical specimens were cut into two; one was fixed with 10% buffered formalin to prepare hematoxylin and eosin (H&E)-stained tissue sections, and the other was frozen to prepare lung tissue lysates. When an H&E-stained specimen was diagnosed as being emphysematous consistently by two pathologists, the patient was included in the present study as an "emphysematous lung" case. In contrast, when two pathologists consistently diagnosed that an H&E-stained specimen had little pathologic changes, the patient was included as a "normal lung" case. Frozen lung tissues from either case group were broken into pieces, and were lysed in a buffer containing 50 mM Tris-HCl (pH 8.0), 150 mM NaCl, 1% Triton X-100, and a protease inhibitor cocktail (Sigma-Aldrich). Insoluble components containing the nuclei were removed by centrifugation, and the supernatant was used as a lung tissue lysate. All patients provided written informed consent to participate in this study, and our institutional review board approved the experimental protocol (approval number, Eki-350). Normal (n = 3) and emphysematous (n = 3) lungs were also obtained from autopsied patients who did not have lung cancer and died in Kinki University Hospital (Osaka, Japan). The

tissue lysates were subjected to Western blot analyses. The Ethics Committee of Kinki University approved the experimental protocol (25-088).

Western blot analysis

Western blot analyses were conducted, and immunoreactive band intensities were quantified using NIH ImageJ software, as described previously.[3]

Plasmid constructs

To express αCTF exogenously on the cell membrane, the polymerase chain reaction (PCR)-based overlap extension method was applied to a plasmid vector expressing the full-length human CADM1 (pCX4bsr-CADM1)[4] using two primer sets: A, forward, 5′-AGTCTGAGGGCAGGTGCCCGACAT-3′ (annealing to the 5′ untranslated region immediately upstream of the signal peptide start codon), and reverse, 5′-*cgagccttcttcacctgcCAG*ATTCTGCCCATCACCTGTG-3′ (the underlined lower-case and upper-case portions correspond to the N-terminal codon of αCTF and the C-terminal codon of the signal peptide sequence, respectively); and B, forward, 5′-CTGGCAGGTGAAGAAGGCTCG-3′ (complementary to the italicised portion of set A reverse primer), and reverse, 5′-CAGTTGGACACCTCATTGGAAC-3′ (annealing to the 3′ untranslated region of CADM1). The final PCR product encoded a large-deletion form of CADM1, in which the signal peptide (amino acids 1–44) was ligated upstream of αCTF (amino acids 363–442) with a three amino acid (45–47) insertion (numbered according to human CADM1, http://www.uniprot.org/uniprot/Q9BY67). This PCR product was inserted into pTA2 TA-cloning vector (Toyobo, Osaka, Japan). After amplification, the insert was excised by *Eco*RI digestion, and ligated to pCX4bsr vector

via the *Eco*RI site (pCX4bsr-SP-αCTF). Directional ligation was confirmed by sequencing.

When the αCTF intracytoplasmic domain amino acid sequence was analysed with a computer-assisted algorithm WoLF PSORT (http://wolfpsort.seq.cbrc.jp/), the domain was predicted to localise to mitochondria. According to this algorithm, we designed a mutant form of αCTF with an intracytoplasmic domain that was predicted to localise not to mitochondria but to the cytosol (supplementary figure S3). To obtain this mutant, in the pCX4bsr-SP-αCTF construct, a portion of the αCTF cytoplasmic region, 5′-gcc gat gac gca gca gac gca gac aca gct ata atc aat gca gaa gga gga cag-3′ encoding ADDAADADTAIINAEGGQ (amino acids 414–431, 18 amino acids long), was mutated to 5′- ggc ggt ggc gga gga ggc gga ggc gca ggt gta atc aat gca gaa gga-3′ encoding GGGGGGGGAGGINAEG (16-amino acid-long) using multiple steps of site-directed mutagenesis (pCX4bsr-SP-αCTFmut). These two vector constructs were used as templates in PCR together with a primer set: forward, 5′-CCCAAGCTTgcaGGTGAAGAAGGCTCGATCAGG-3′ (containing a *Hind*III site, underlined, immediately upstream of the N-terminal codon of αCTF, lower-case); and reverse, 5′-GACAAACGCACACCGGCCTTATTCC-3′ (annealing to the vector sequence downstream of the multiple cloning site). Two PCR products were digested by *Eco*RI and *Hind*III digestion and then were inserted into the p3xFLAG-CMV-9 vector (Sigma-Aldrich) via *Hind*III and *Eco*RI sites (p3xFLAG-αCTF and p3xFLAG-αCTFmut). The absence of mutation was verified by sequencing.

Transfection

Cells were grown to 60–70% confluence, and were transfected with the indicated plasmid vectors using the Lipofectamine LTX and Plus reagents (Invitrogen) according to the manufacturer's instructions.

Immunofluorescence and mitochondrial labelling

Cells were grown in coverslip-like-bottomed culture dishes of a 35-mm diameter (μ-Dish; ibidi, Munich, Germany), and were either treated with a mixture of PMA (200 nM) and trypsin (0.0125% w/v) or transfected as described above, or left untreated. After 2 days of transfection or 20 min of treatment, cells were incubated in RPMI-1640 medium containing 10% FBS and 200 nM Mitotracker (Molecular Probes, Eugene, OR, USA) for 30 min, and washed with PBS. Then cells were fixed with ice-cold methanol for 10 min, blocked with 2% bovine serum albumin for 30 min, and incubated with the anti-CADM1 antibody overnight at 4°C. Cells were washed three times, and incubated with an Alexa Fluor 488-conjugated anti-rabbit IgG antibody for 2 h at 4°C for visualisation. Stained images were captured using a confocal laser microscope (LSM510 Meta; Carl Ziess, Oberkochen, Germany). Intensity correlation between red and green fluorescence was quantified using the Colocalization Analysis plugin of ImageJ software, and the overlap coefficient was calculated for each image. The mean and standard deviation (SD) of the overlap coefficient were calculated from more than 10 images per each type of cells.

Double immunofluorescence of lung sections were performed as described previously.[5] Briefly, paraffin-embedded lung sections were deparaffinised, rehydrated, antigen retrieved by microwave heating in 10 mM citrate buffer (pH 6.0), blocked with 2% bovine serum albumin, and incubated with a mixture of antibodies against CADM1 and

mitochondria (clone 113-1) overnight at 4°C. Sections were incubated with an Alexa Fluor 488-conjugated anti-rabbit IgG and an Alexa Fluor 568-conjugated anti-mouse IgG antibody for 2 h, followed by nuclear counterstaining with DAPI. Triple stained images were captured using a confocal laser microscope (AZ-C2 plus; Nikon, Tokyo, Japan), and merged on the differential interference contrast image. Alveolar epithelial cells were identifiable by CADM1 membranous immunostaining (green). CADM1 immunostaining was occasionally detected in the cytoplasm, and appreciably colocalised with mitochondrial immunostaining (red). The number (%) of cells with this colocalisation signal (yellow) was counted in 100 alveolar epithelial cells for each case, and the mean and SD were calculated from the results of four cases for each of normal and emphysematous lungs.

Cell fractionation

Cells (2.1×10^7) grown in culture dishes were treated with trypsin (0.25% v/w), suspended in PBS, and collected as two (1×10^6 and 2×10^7) cell pellets by centrifugation. The small cell pellet was lysed in a buffer containing 50 mM Tris-HCl (pH 8.0), 150 mM NaCl, 1% Triton X-100, and a protease inhibitor cocktail (Sigma-Aldrich). Insoluble components containing the nuclei were removed by centrifugation, and the supernatant was used as a whole cytoplasmic lysate. The large cell pellet was separated into cytosolic and mitochondrial fractions using a Mitochondria Isolation Kit for Mammalian Cells (Thermo Scientific, Waltham, MA, USA) according to the manufacturer's instructions.

Mitochondrial membrane potential

JC-1 dye (Molecular Probes, Life Technologies) was used to measure mitochondrial inner membrane potential (ΔΨm) in living cells. When ΔΨm is high, JC-1 accumulates in the mitochondria, forming aggregates that fluoresce red. When ΔΨm is low, JC-1 exists in the cytoplasm as monomers that fluoresce green. The ratio of red-to-green fluorescence is proportional to ΔΨm. Cells were grown to 60–70% confluence in coverslip-like-bottomed culture dishes of a 35-mm diameter (μ-Dish; ibidi) and were transfected or treated as indicated. At the indicated time points, cells were incubated in RPMI1640 containing 10% FBS and 1.0 μg/mL JC-1 at 37°C for 20 min, rinsed twice with PBS, and incubated in RPMI1640 containing 10% FBS for 10 min. Then, the cell culture was transferred into a temperature-controlled (37°C) chamber unit (CZL-3; Carl Zeiss) that was supplied with 5% CO_2 and placed on an automated stage of an LSM510 Meta confocal microscope (Carl Zeiss). About 10–20 cells were observed per field of view using a 63× objective lens, and total intensities of red (excitation, 550 nm; emission, 600 nm) and green (excitation, 485 nm; emission, 535 nm) fluorescence per field were measured with a morphometric analysis tool attached to the microscope computer. Approximately 20 fields of view were analysed for each experimental group, and the mean and SD of the red/green fluorescence intensity ratio were calculated. Experiments were repeated independently three times, with essentially similar results.

TUNEL assay

TUNEL assays were conducted on cultured cells and formalin-fixed, paraffin-embedded lung sections using the In Situ Cell Death Detection Kit (Roche Applied Science, Upper Bavarie, Germany) according to the manufacturer's instructions. Briefly, cells were grown to 60–70% confluence in μ-Dishes (ibidi) and transfected with indicated vectors

or left untransfected. After 48 h, cells were fixed with 4% paraformaldehyde, permeabilised with 0.1% Triton X-100 in 0.1% sodium citrate (pH7.4), and then were incubated with the TUNEL reaction mixture containing terminal deoxynucleotidyl transferase and FITC-labelled dUTP for 1 h at 37°C, followed by nuclear counterstaining with DAPI. E-cadherin immunofluorescence was performed for lung sections as described previously[6] prior to the assay. Briefly, thin sections were prepared from paraffin-embedded tissues, deparaffinised, rehydrated, autoclaved in 10 mM citrate buffer (pH 6.0) for 20 min at 121°C, blocked with 2% bovine serum albumin, and incubated with the anti-E-cadherin antibody for 2 h, followed by an incubation with an Alexa Fluor 568-conjugated anti-mouse IgG antibody for 2 h. Then, sections were incubated with the TUNEL reaction mixture containing terminal deoxynucleotidyl transferase and FITC-labelled dUTP, followed by nuclear counterstaining with DAPI. Double-stained cultured cells and triple-stained lung sections were observed through a fluorescence microscope (Axio Observer D1; Carl Zeiss). When a cell had TUNEL signals within the DAPI nuclear stain, the cell was deemed TUNEL-positive. Alveolar epithelial cells in lung sections were identified by membranous staining for E-cadherin, and the number of TUNEL-positive cells was counted in 500 alveolar epithelial cells from three or four sections for each case. Data are expressed as mean ± SD of the proportion of TUNEL-positive cells for each experimental group.

Reverse transcription-PCR

The methods of RNA extraction, reverse transcription, and PCR to detect CADM1 isoforms were essentially identical to those described previously,[1] except that an

oligonucleotide 5'-AAAATAGCGCCCCAGAATGATGAGC-3' was used as a reverse primer in PCR to amplify human CADM1 mRNA.

Statistical analysis

Statistical differences among experimental groups were analysed using the Mann–Whitney *U*-test for the quantified Western blot data and proportions of TUNEL-positive cells and alveolar epithelial cells with CADM1-mitochondria colocalisation, and Student's *t*-test for JC-1 green/red fluorescence intensity ratios. In multiple testing, all pairwise comparisons were Bonferroni corrected, with the allowance being set < 0.05. The data subjected to *t*-tests were confirmed to meet the normality assumption by the F-test. Correlations were analysed using the Spearman's rank test. A P value ≤ 0.05 was considered significant.

REFERENCES

1. Hagiyama M, Ichiyanagi N, Kimura KB, et al. Expression of a soluble isoform of cell adhesion molecule 1 in the brain and its involvement in directional neurite outgrowth. *Am J Pathol* 2009;174:2278-89.
2. Kuramochi M, Fukuhara H, Nobukuni T, et al. TSLC1 is a tumor-suppressor gene in human non-small-cell lung cancer. *Nat Genet* 2001;27:427-30.
3. Mimae T, Okada M, Hagiyama M, et al. Upregulation of notch2 and six1 is associated with progression of early-stage lung adenocarcinoma and a more aggressive phenotype at advanced stages. *Clin Cancer Res* 2012;18:945-55.
4. Ito A, Hagiyama M, Mimae T, et al. Expression of cell adhesion molecule 1 in malignant pleural mesothelioma as a cause of efficient adhesion and growth on mesothelium. *Lab Invest* 2008;88:504-14.
5. Koma Y, Furuno T, Hagiyama M, et al. Cell adhesion molecule 1 is a novel pancreatic-islet cell adhesion molecule that mediates nerve-islet cell interactions. *Gastroenterology* 2008;134:1544-54.
6. Ito A, Okada M, Uchino K, et al. Expression of the TSLC1 adhesion molecule in pulmonary

epithelium and its down-regulation in pulmonary adenocarcinoma other than bronchioloalveolar carcinoma. *Lab Invest* 2003;83:1175-83.

Figure legends

Supplementary figure S1

Histological diagnosis of “normal” and “emphysematous” lungs.

Formalin-fixed, paraffin-embedded lungs were cut into sections, and stained with hematoxylin and eosin (H&E). Representative histological pictures of “normal” and “emphysematous” lungs are shown in the upper and lower panels, respectively. Bar = 100 μm.

Supplementary figure S2

Graphs with band intensity ratios of E-cadherin/β-actin and CADM1 full-length/β-actin on the X- and Y-axes, respectively. These two ratios were well approximated as linear in both normal (left) and emphysematous (right) lungs. Correlation and statistical significance were analysed by the Spearman’s rank test, and R^2 and *P*-values are shown. White circles, normal lung non-smoker; triangles, normal lung smoker; black circles, emphysematous lung smoker.

Supplementary figure S3

Schematic presentation of the structure of αCTF and its mutant form αCTFmut. Mutations in αCTFmut, amino acid substitution and deletion (–), are shown with single-letter codes. Conserved amino acid residues are shaded. Amino acid residues positioned at the start and end of structural domains are numbered according to; http://www.uniprot.org/uniprot/Q9BY67. Arrows indicate the position of α-, β-, and γ-shedding that produce αCTF, βCTF, and ICD, respectively. A hatched rectangle indicates the C-terminal region recognized by the CADM1 antibody used. SP, signal peptide; TM,

transmembrane domain; 4.1-BM, protein 4.1-binding motif; PDZ-BM, PDZ domain-binding motif.

Supplementary figure S4

Protein levels of full-length CADM1 and αCTF in NCI-H441 cells. **A.** Western blot analyses of human lung cancer cell lines, NCI-H441, A549 and NCI-H596, and normal lungs for CADM1. The protein levels of full-length CADM1 in these cell lines and tissues were well correlated with their mRNA levels assessed by Northern blot analyses shown in our past work.[2] Note that CADM1 is as abundant in NCI-H441 cells as in normal lungs, when normalized to β-actin. Considering that lung tissues contain CADM1-negative cells, it seems that full-length CADM1 in NCI-H441 cells is certainly lower than in normal lung epithelial cells in vivo. **B.** Western blot analyses of NCI-H441 cells transfected with αCTF cDNA for CADM1. Protein lysates were prepared from cells transfected individually three times (corresponding to lanes 1 to 3). The ratios of αCTF to full-length CADM1 were plotted with grey circles in **C**, together with the ratios in emphysematous lungs (closed circles; identical to the plot of figure 1C). A *P* value was calculated by the Mann–Whitney *U*-test.

Supplementary figure S5

Exogenous expression of FLAG-tagged αCTF and αCTFmut in NCI-H441 cells.
Upper panel: NCI-H441 cells were untransfected (left) or transfected with p3xFLAG-αCTF (middle) or p3xFLAG-αCTFmut (right), and were fractionated into cytosolic (CS) and mitochondrial (Mit) fractions. Whole cytoplasmic lysates (CP) were extracted from aliquots of the cells. These lysates and fractions were analysed with Western blotting

using an anti-FLAG antibody. White and black arrows indicate FLAG-tagged αCTF and αCTFmut, respectively. Open and closed arrows indicate FLAG-tagged αCTF and αCTFmut, respectively. (This result was obtained by reprobing the blots in Fig. 5 of the main text.)

Lower panel: The blots were stained with silver reagents (Wako Pure Chemical Industries, Osaka, Japan) to indicate the protein loading per lane.

Supplementary figure S6

Differential interference contrast images of NCI-H441 cells stained with JC-1 dye. These pictures correspond to the differential interference contrast images of NCI-H441 cells shown in Fig. 6A of the main text. As described in the Fig. 6A legend, NCI-H441 cells were untransfected (upper) or transfected with pCX4bsr-SP-αCTF (middle) or pCX4bsr-SP-αCTFmut (lower) and were stained with JC-1 dye 48 h later. Differential interference contrast images were captured by a confocal laser microscope. Green and red fluorescence images are shown in Fig. 6A of the main text. Bar = 20 μm.

Supplementary figure S7

CADM1 expression in lungs without lung cancer. Normal (n = 3) and emphysematous (n = 3) lungs were removed from autopsied patients who did not have lung cancer, and their protein lysates were subjected to Western blot analyses for CADM1. The blots were reprobed with an anti-β-actin antibody to indicate protein loading per lane. Patient characteristics are as follows.

Lung histology	Patient No.	Age	Sex	Cause of death
Normal	1	43	M	Infectious colitis
	2	72	M	Aplastic anemia
	3	76	M	Hepatocellular carcinoma
Emphysematous	1	71	M	Gastric cancer
	2	62	F	Peritoneal carcinoma
	3	72	M	Pancreatic cancer

Supplementary figure S8

CADM1 isoforms expressed in human lungs and NCI-H441 cells. Total RNAs extracted from lung tissues of cases indicated and NCI-H441 cells were reverse transcribed and PCR-amplified using a primer set encompassing the CADM1 extracellular juxtamembrane region, susceptible to alternative splicing. The PCR products were electrophoresed on 3% agarose gels, together with CADM1 isoform size markers (rightmost lane). L, 100 base pair (bp) ladder. RNAs were also PCR-amplified using a primer set for G3PDH to indicate RNA loading per lane.

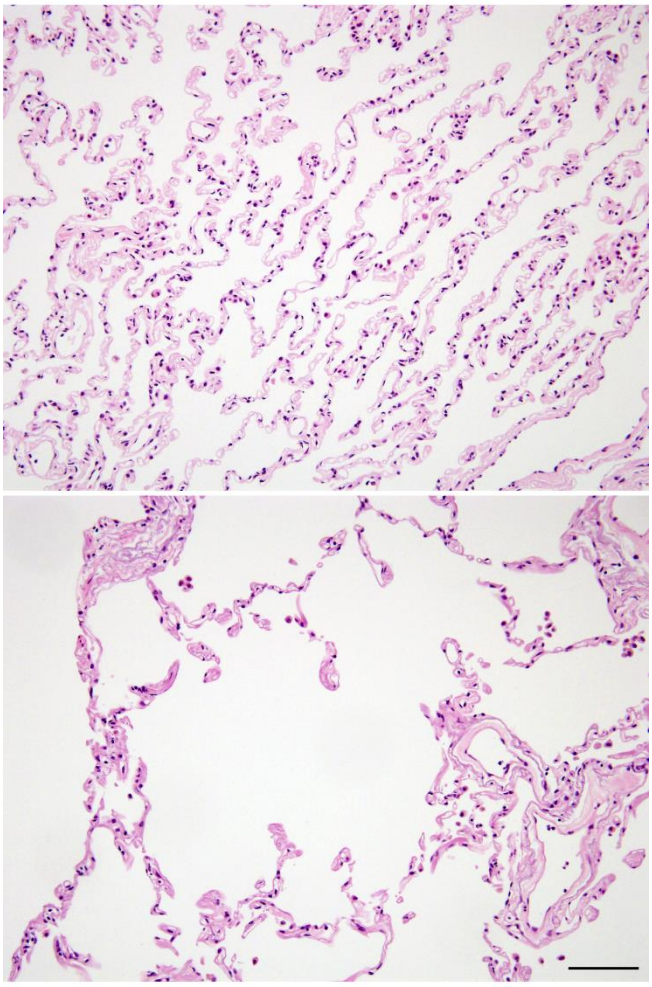

Supplementary figure S1

Histological diagnosis of “normal” and “emphysematous” lungs.

Formalin-fixed, paraffin-embedded lungs were cut into sections, and stained with hematoxylin and eosin (H&E). Representative histological pictures of “normal” and “emphysematous” lungs are shown in the upper and lower panels, respectively. Bar = 100 μm.

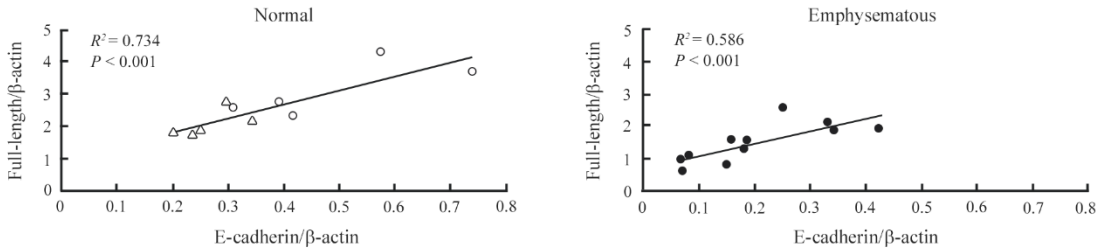

Supplementary figure S2

Graphs with band intensity ratios of E-cadherin/β-actin and CADM1 full-length/β-actin on the X- and Y-axes, respectively. These two ratios were well approximated as linear in both normal (left) and emphysematous (right) lungs. Correlation and statistical significance were analysed by the Spearman's rank test, and R^2 and *P*-values are shown. White circles, normal lung non-smoker; triangles, normal lung smoker; black circles, emphysematous lung smoker.

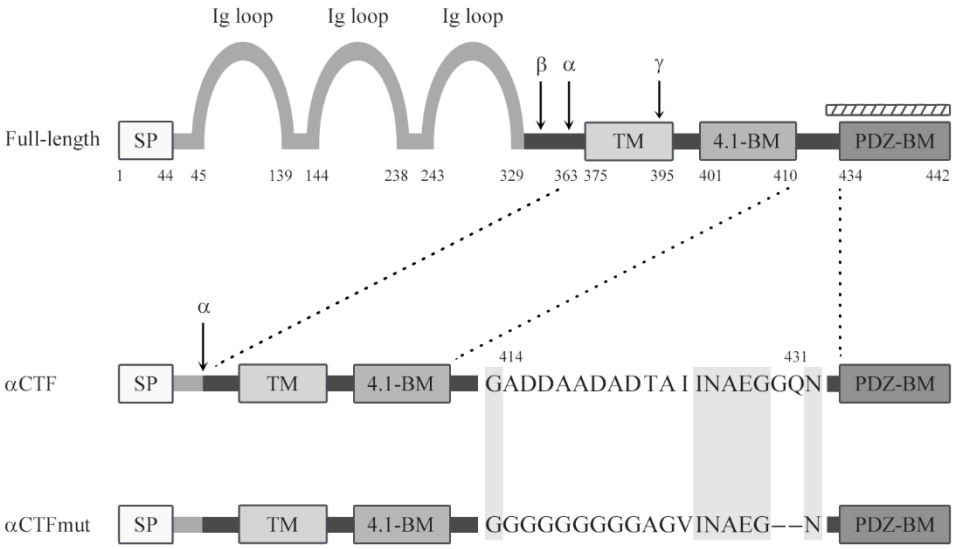

Supplementary figure S3

Schematic presentation of the structure of αCTF and its mutant form αCTFmut. Mutations in αCTFmut, amino acid substitution and deletion (–), are shown with single-letter codes. Conserved amino acid residues are shaded. Amino acid residues positioned at the start and end of structural domains are numbered according to; http://www.uniprot.org/uniprot/Q9BY67. Arrows indicate the position of α-, β-, and γ-shedding that produce αCTF, βCTF, and ICD, respectively. A hatched rectangle indicates the C-terminal region recognized by the CADM1 antibody used. SP, signal peptide; TM, transmembrane domain; 4.1-BM, protein 4.1-binding motif; PDZ-BM, PDZ domain-binding motif.

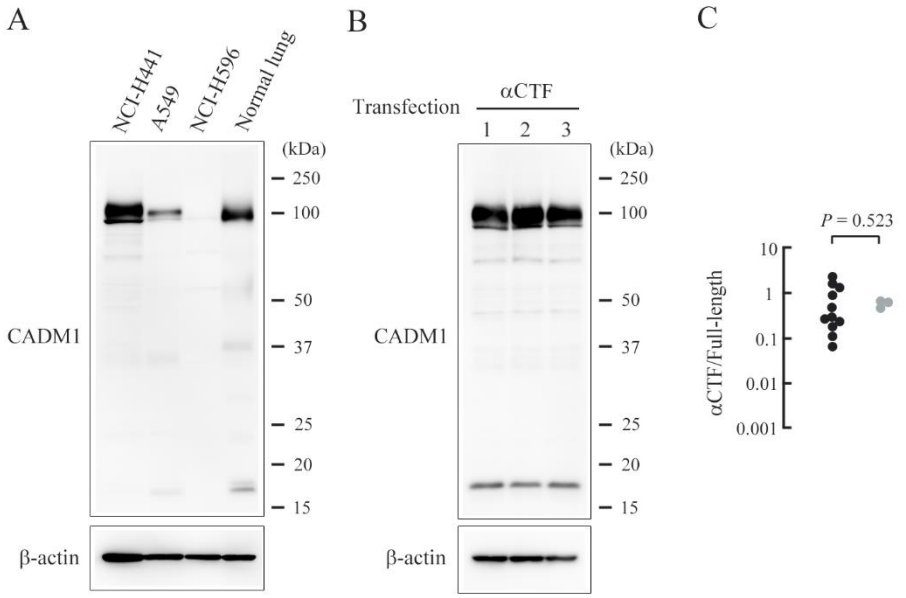

Supplementary figure S4

Protein levels of full-length CADM1 and αCTF in NCI-H441 cells. **A.** Western blot analyses of human lung cancer cell lines, NCI-H441, A549 and NCI-H596, and normal lungs for CADM1. The protein levels of full-length CADM1 in these cell lines and tissues were well correlated with their mRNA levels assessed by Northern blot analyses shown in our past work.[2] Note that CADM1 is as abundant in NCI-H441 cells as in normal lungs, when normalized to β-actin. Considering that lung tissues contain CADM1-negative cells, it seems that full-length CADM1 in NCI-H441 cells is certainly lower than in normal lung epithelial cells in vivo. **B.** Western blot analyses of NCI-H441 cells transfected with αCTF cDNA for CADM1. Protein lysates were prepared from cells transfected individually three times (corresponding to lanes 1 to 3). The ratios of αCTF to full-length CADM1 were plotted with grey circles in **C**, together with the ratios in emphysematous lungs (closed circles; identical to the plot of figure 1C). A *P* value was calculated by the Mann–Whitney *U*-test.

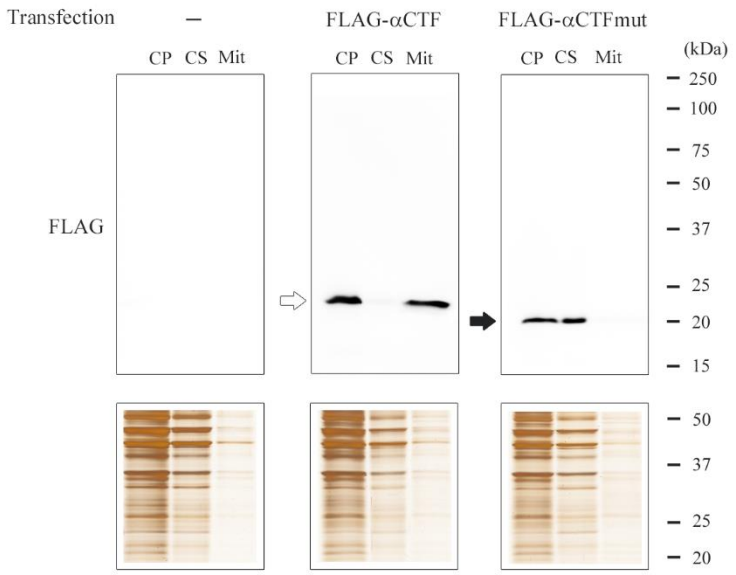

Supplementary figure S5

Exogenous expression of FLAG-tagged αCTF and αCTFmut in NCI-H441 cells.

Upper panel: NCI-H441 cells were untransfected (left) or transfected with p3xFLAG-αCTF (middle) or p3xFLAG-αCTFmut (right), and were fractionated into cytosolic (CS) and mitochondrial (Mit) fractions. Whole cytoplasmic lysates (CP) were extracted from aliquots of the cells. These lysates and fractions were analysed with Western blotting using an anti-FLAG antibody. White and black arrows indicate FLAG-tagged αCTF and αCTFmut, respectively. Open and closed arrows indicate FLAG-tagged αCTF and αCTFmut, respectively. (This result was obtained by reprobing the blots in Fig. 5 of the main text.)

Lower panel: The blots were stained with silver reagents (Wako Pure Chemical Industries, Osaka, Japan) to indicate the protein loading per lane.

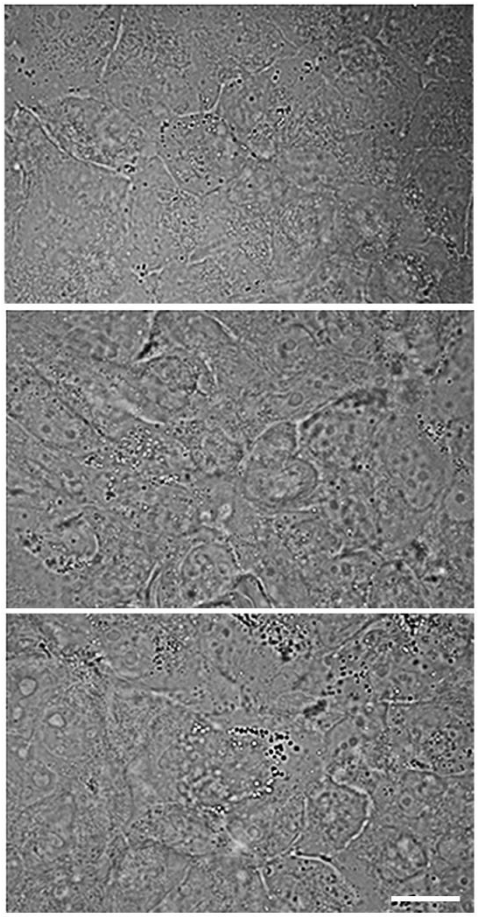

Supplementary figure S6

Differential interference contrast images of NCI-H441 cells stained with JC-1 dye.

These pictures correspond to the differential interference contrast images of NCI-H441 cells shown in Fig. 6A of the main text. As described in the Fig. 6A legend, NCI-H441 cells were untransfected (upper) or transfected with pCX4bsr-SP-αCTF (middle) or pCX4bsr-SP-αCTFmut (lower) and were stained with JC-1 dye 48 h later. Differential interference contrast images were captured by a confocal laser microscope. Green and red fluorescence images are shown in Fig. 6A of the main text. Bar = 20 μm.

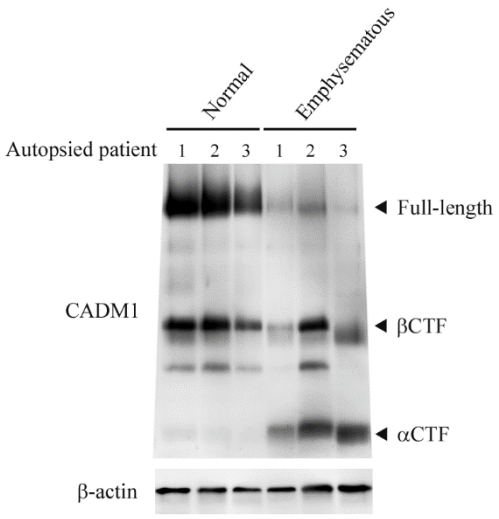

Supplementary figure S7

CADM1 expression in lungs without lung cancer. Normal (n = 3) and emphysematous (n = 3) lungs were removed from autopsied patients who did not have lung cancer, and their protein lysates were subjected to Western blot analyses for CADM1. The blots were reprobed with an anti-β-actin antibody to indicate protein loading per lane. Patient characteristics are as follows.

Lung histology	Patient No.	Age	Sex	Cause of death
Normal	1	43	M	Infectious colitis
	2	72	M	Aplastic anemia
	3	76	M	Hepatocellular carcinoma
Emphysematous	1	71	M	Gastric cancer
	2	62	F	Peritoneal carcinoma
	3	72	M	Pancreatic cancer

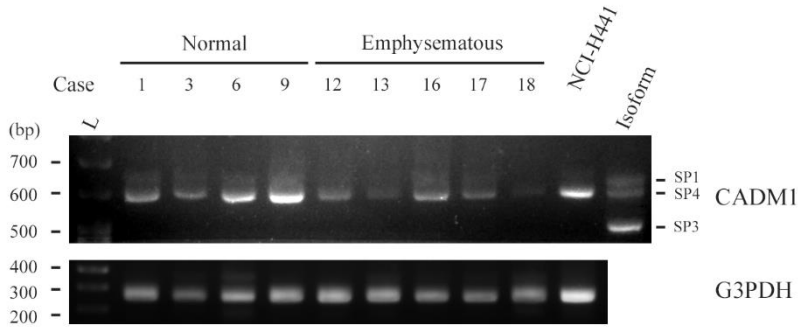

Supplementary figure S8

CADM1 isoforms expressed in human lungs and NCI-H441 cells. Total RNAs extracted from lung tissues of cases indicated and NCI-H441 cells were reverse transcribed and PCR-amplified using a primer set encompassing the CADM1 extracellular juxtamembrane region, susceptible to alternative splicing. The PCR products were electrophoresed on 3% agarose gels, together with CADM1 isoform size markers (rightmost lane). L, 100 base pair (bp) ladder. RNAs were also PCR-amplified using a primer set for G3PDH to indicate RNA loading per lane.